



<http://www.diva-portal.org>

Preprint

This is the submitted version of a paper published in *Journal of Medicinal Chemistry*.

Citation for the original published paper (version of record):

Hofström, C., Altai, M., Honarvar, H., Strand, J., Malmberg, J. et al. (2013)
HAHAHA, HEHEHE, HIIIIHI, or HKHKHK: Influence of Position and Composition of
Histidine Containing Tags on Biodistribution of [^{99m}Tc(CO)₃]⁺-Labeled Affibody Molecules.
Journal of Medicinal Chemistry, 56(12): 4966-4974
<http://dx.doi.org/10.1021/jm400218y>

Access to the published version may require subscription.

N.B. When citing this work, cite the original published paper.

This document is the unedited Author's version of a Submitted Work that was subsequently accepted for publication in *Journal of Medicinal Chemistry* © American Chemical Society after peer review. To access the final edited and published work see

Permanent link to this version:

<http://urn.kb.se/resolve?urn=urn:nbn:se:uu:diva-203052>

This document is the unedited Author's version of a Submitted Work that was subsequently accepted for publication in Journal of Medicinal Chemistry © American Chemical Society after peer review. To access the final edited and published work see

Hofström C, Altai M, Honarvar H, Strand J, Malmberg J, Hosseinimehr SJ, Orlova A, Gräslund T, Tolmachev V. HAHAHA, HEHEHE, HIIHHI, or HKHKHK: influence of position and composition of histidine containing tags on biodistribution of [(99m)Tc(CO)₃]⁽⁺⁾-labeled affibody molecules. J Med Chem. 2013 Jun 27;56(12):4966-74. doi: 10.1021/jm400218y

<http://pubs.acs.org/doi/abs/10.1021/jm400218y>

HAHAAA, HEHEHE, HIIHHI or HKHKHK: influence of position and composition of histidine containing tags on biodistribution of [^{99m}Tc(CO)₃]⁺- labeled affibody molecules.

Camilla Hofström¹, Mohamed Altai², Hadis Honarvar², Joanna Strand², Jennie Malmberg³, Seyed Jalal Hosseinimehr^{2,4}, Anna Orlova³, Torbjörn Gräslund^{1*}, Vladimir Tolmachev².

¹KTH Royal Institute of Technology, School of Biotechnology, Division of Protein Technology, Stockholm, Sweden;

²Division of Biomedical Radiation Sciences, Rudbeck Laboratory, Uppsala University, Uppsala, Sweden;

³Preclinical PET Platform, Department of Medicinal Chemistry, Uppsala University, Uppsala, Sweden;

⁴Department of Radiopharmacy, Faculty of Pharmacy, Mazandaran University of Medical Sciences, Sari, Iran

ABSTRACT

Engineered affibody molecules can be used for high contrast in vivo molecular imaging. Extending a recombinantly produced HER2 binding affibody molecule with a hexa-histidine tag allows for convenient purification by immobilized metal-ion affinity chromatography and labeling with [$^{99m}\text{Tc}(\text{CO})_3$] $^+$ but increases radioactivity uptake in the liver. To investigate the impact of charge, lipophilicity and position on biodistribution, ten variants of a histidine-based tag was attached to a HER2 binding affibody molecule. The biochemical properties and the HER2 binding affinity appeared to be similar for all variants. In vivo, positive charge promoted liver uptake. For N-terminally placed tags, lipophilicity promoted liver uptake and decreased kidney uptake. Kidney uptake was higher for C-terminally placed tags compared to their N-terminal counterparts. The variant with the amino acid composition HEHEHE placed in the N-terminus gave the lowest non-specific uptake.

INTRODUCTION

A promising approach to treat disseminated cancer is a specific delivery of cytotoxic agents to the tumor cells, i.e. targeting therapy. Targeting can be achieved by attachment of the cytotoxic agent to an affinity probe that specifically recognizes tumor-associated phenotypic abnormalities.

Often, the molecular targets on the tumor cells are transmembrane receptor tyrosine kinases (RTKs) regulating proliferation, differentiation, apoptosis, motility and angiogenesis.¹ Abnormal expression of a RTK (e.g. over-expression or expression of mutated forms) is often predictive for response to the targeting therapy. The use of radionuclide molecular imaging for detection of abnormal expression of a RTK therefore has the potential to improve patient stratification for successful targeting therapy.²

Affibody molecules are a novel class of affinity proteins that have been generated to target a number of different proteins with low nanomolar or even subnanomolar affinities.³ They are derived from a modified version of the triple-helical B-domain of staphylococcal protein A. To generate affibody molecules interacting with a desired target, phage display selection from a combinatorial library followed by affinity maturation is typically performed. The library consists of variants of the modified version of the B-domain where 13 surface-exposed amino acids in helix 1 and 2 (near the N-terminus) have been combinatorially varied.³ Affibody molecules with subnanomolar affinity to several RTKs, such as HER2,⁴ EGFR,⁵ HER3,⁶ PDGFR β ,⁷ and IGF-1R⁸ have been identified. When used for radionuclide molecular imaging, the small size of the affibody molecule (approx. 7 kDa) leads to rapid extravasation and tissue penetration and also to rapid clearance of non-bound tracer molecules from blood and non-specific compartments. In combination with high affinity, this creates the preconditions for high-contrast imaging of RTKs in vivo. Indeed, preclinical studies have shown the high potential of radiolabeled affibody

molecules as imaging agents.⁹ Two clinical studies also confirmed the potential of affibody-based imaging agents for visualization of HER2-expressing metastases in patients with disseminated breast cancer.^{10,11}

Biodistribution and targeting properties of radiolabeled affinity probes relies on several factors including probe size, target affinity and specificity, labeling stability, lipophilicity and charge.¹² Understanding how these factors affect biodistribution is important to minimize unspecific uptake and processing of the probe. Sensitivity of imaging depends on many parameters including absolute tumor uptake and contrast, where contrast in turn is affected by the tumor-to-normal tissue ratios. Thus, minimization of the uptake of an imaging probe in normal tissues is as important as maximizing its uptake in tumors. Previous studies have demonstrated that the properties of the radionuclide in combination with a chelator or linker for attachment to the targeting protein can substantially influence radioactivity uptake.¹²

^{99m}Tc ($T_{1/2} = 6\text{h}$, $E_{\gamma} = 140.5\text{ keV}$) is a commonly used radionuclide for molecular imaging applications due to its photon energy (nearly ideal for SPECT imaging), low cost, excellent availability and low absorbed dose burden to the patient. Also, recent developments of SPECT/CT hybrid instruments now allow for unprecedented imaging quality using ^{99m}Tc.¹³ Several different peptide based radionuclide chelators for conjugation of ^{99m}Tc to affibody molecules have been investigated.¹⁴⁻¹⁷ The use of peptide-based chelators provides an opportunity for their direct incorporation in the peptide sequence of the targeting protein by genetic engineering, thus excluding an additional conjugation step. One of the peptide-based chelators that has been used to conjugate ^{99m}Tc to affibody molecules is the hexahistidine tag (H₆-tag), which allows facile labeling with [^{99m}Tc(CO)₃]⁺.¹⁸ The H₆-tag may also be used for convenient purification of the affibody molecule by immobilized metal-ion affinity chromatography (IMAC)

after recombinant production. However, the H₆-tag altered the biodistribution of the probe with an increase of radioactivity uptake in the liver compared to the same construct lacking a H₆-tag and labeled by other methods.¹⁴ Unspecific radioactivity uptake in the liver is problematic since the liver is a common metastatic site of many types of cancer. From other studies, it was found that substitution of only a few amino acids in the chelating part of an affibody molecule can dramatically alter its biodistribution.^{16,17} This prompted the search for alterations to the placement and composition of the His₆-tag that would lead to decreased uptake of radioactivity in the liver. The proposed structure of the [^{99m}Tc(CO)₃]⁺-His₆-tag complex suggests that the peptide motif H-X-H is responsible for chelation of technetium, i.e. every second histidine is involved in the chelation (Figure 1).¹⁹ It implies that labeling of modified histidine-based tags with the format: H-X-H-X-H-X, where X is a variable amino acid, would be allowed. To explore this hypothesis we previously devised and attached a HEHEHE-tag ((HE)₃-tag) to the HER2-binding affibody molecule Z_{HER2:342} and found that it allowed purification by IMAC and stable and efficient labeling with [^{99m}Tc(CO)₃]⁺.²⁰ A comparative biodistribution of Z_{HER2:342} extended with either a H₆-tag or the (HE)₃-tag showed dramatic differences, where the liver uptake was decreased ten-fold for the (HE)₃-tag containing probe. In the same study, repositioning of the H₆-tag from the N- to C-terminus was found to decrease liver uptake by two-fold. It has to be noted that although that study has demonstrated that position and composition of a histidine tag strongly influences the biodistribution of affibody molecules, the choice of creating the variant with a N-terminal (HE)₃-tag was based mainly on intuition. The influence of charge and lipophilicity of the side-chains in histidine containing peptide-based chelators on biodistribution have not previously been investigated.

In this study, the goal was to examine the behavior of an affibody molecule, extended with a tag with the amino acid sequence H-X-H-X-H-X, by systematically varying charge, lipophilicity and

position of the tag. The amino acid X was histidine, glutamic acid, lysine, alanine or isoleucine (Figure 1). Lysine was selected because it is as hydrophilic as glutamic acid, but has an opposite charge at physiological conditions. The use of alanine and isoleucine allowed for elucidation of the effect of increased lipophilicity. Based on the calculated differences in net charge and lipophilicity of the tags (Figure 1), it was expected that they would lead to differences in the biodistribution of the probe. The position of the tags was varied by placement in the N- or C-terminus. The variants were labeled with $[^{99m}\text{Tc}(\text{CO})_3]^+$ and the chelate stability and biodistribution of the labeled probes was investigated.

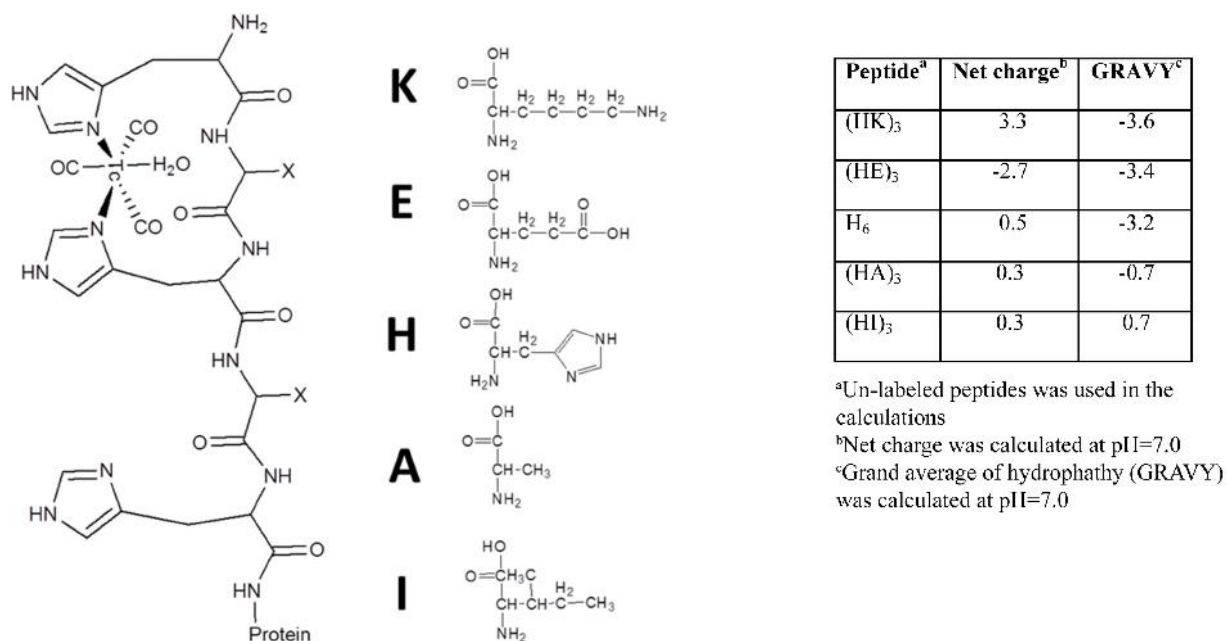


Figure 1. Proposed structure of $[^{99m}\text{Tc}(\text{CO})_3]^+$ -labeled histidine-containing tags and calculated biochemical properties of the free peptides.

RESULTS

Production, purification and characterization of the affibody molecules

The affibody molecule Z_{HER2:342}, extended with different (HX)₃-tags, was produced in *Escherichia coli* and purified by IMAC followed by reverse-phase HPLC (RP-HPLC) as previously described.²⁰ Eluted fractions after the RP-HPLC-step contained essentially a single protein of expected molecular weight when analyzed by SDS-PAGE (data not shown). The purified proteins were stable at mg/mL-concentrations in phosphate buffered saline (PBS) except for (HI)₃-Z_{HER2:342}, which precipitated at concentrations higher than 2 mg/mL. The biochemical properties of the variants were investigated and the results are summarized in Table 1. Their molecular masses were determined by LC-MS and the obtained values correlated well (within the accuracy of the method) with their corresponding theoretical molecular masses. The constructs were analyzed by RP-HPLC (Figure 2) and the purity ranged from 95% to more than 99% (Table 1). The secondary structure content of the variants was determined by circular dichroism spectroscopy and was found to be similar for all variants. The melting temperatures were determined and ranged from 63 to 65°C (Table 1). The variants displayed similar secondary structure at 20°C before and after heating to 90°C, indicating that they refolded after thermal denaturation, except for (HI)₃-Z_{HER2:342} that precipitated at around 80°C. Its melting temperature could therefore not be determined but its thermal unfolding curve was similar to the other variants until it precipitated.

Table 1: Biochemical characterization of affibody molecules.

	Calculated Mw (Da)	Found Mw (Da)	Melting Temperature (°C)	RP-HPLC Retention (min)	Purity (%)
H ₆ -Z _{HER2:342}	7859	7860	64	18.49	95.7
(HE) ₃ -Z _{HER2:342}	7835	7836	65	18.54	98.5
(HA) ₃ -Z _{HER2:342}	7661	7662	64	18.56	99.4
(HK) ₃ -Z _{HER2:342}	7833	7833	63	18.43	99.6
(HI) ₃ -Z _{HER2:342}	7787	7788	^a ND	19.06	99.4
Z _{HER2:342} -H ₆	7872	7873	63	18.17	99.6
Z _{HER2:342} -(HE) ₃	7848	7849	63	18.28	98.8
Z _{HER2:342} -(HA) ₃	7674	7675	63	18.34	99.4
Z _{HER2:342} -(HK) ₃	7846	7846	64	18.16	99.6
Z _{HER2:342} -(HI) ₃	7800	7801	63	18.87	99.5

^aND = Not Determined

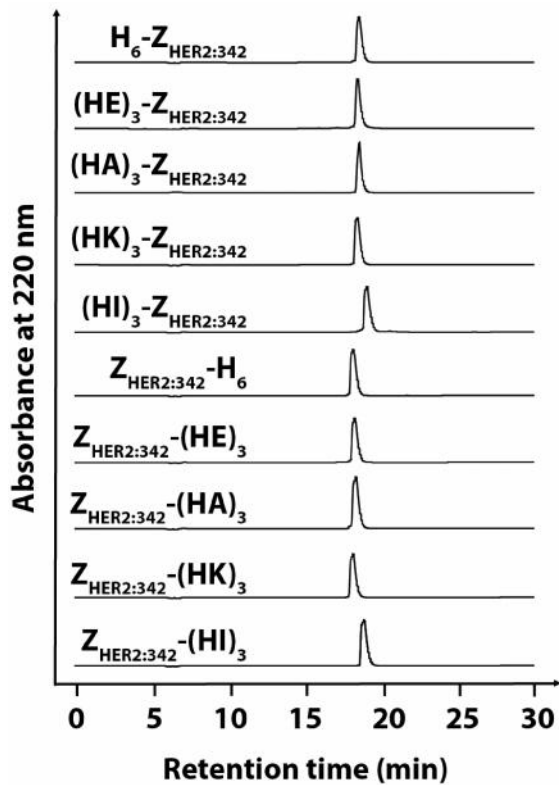


Figure 2. Analytical RP-HPLC analysis of the $(HX)_3$ - $Z_{HER2:342}$ -variants. The x-axis corresponds to retention time after injection and the y-axis corresponds to the absorbance measured at 220 nm.

Analysis of the binding kinetics

Real-time biosensor analysis was performed to investigate if the composition and position of the $(HX)_3$ -tags influenced the kinetic constants of the $Z_{HER2:342}$ -interaction with HER2. The equilibrium dissociation constant, K_D , was found to be similar for all variants ranging between 26 and 88 pM (Table 2). These affinities are somewhat weaker than the previously determined K_D -value of 22 pM for interaction between $Z_{HER2:342}$ and HER2.⁴

Table 2: Measured kinetic constants of the interaction between the affibody molecules and HER2.

	k_a ($M^{-1} s^{-1}$)	k_d (s^{-1})	K_D (pM)
$H_6-Z_{HER2:342}$	2.2×10^6	1.7×10^{-4}	78
$(HE)_3-Z_{HER2:342}$	2.2×10^6	1.9×10^{-4}	88
$(HA)_3-Z_{HER2:342}$	6.1×10^6	1.6×10^{-4}	26
$(HK)_3-Z_{HER2:342}$	5.6×10^6	2.9×10^{-4}	51
$(HI)_3-Z_{HER2:342}$	5.0×10^6	2.5×10^{-4}	51
$Z_{HER2:342}-H_6$	6.9×10^6	2.4×10^{-4}	35
$Z_{HER2:342}-(HE)_3$	6.6×10^6	3.8×10^{-4}	57
$Z_{HER2:342}-(HA)_3$	6.4×10^6	3.7×10^{-4}	58
$Z_{HER2:342}-(HK)_3$	8.2×10^6	3.3×10^{-4}	41
$Z_{HER2:342}-(HI)_3$	8.1×10^6	3.6×10^{-4}	44

Radio-labeling with [$^{99m}\text{Tc}(\text{CO})_3$] $^+$

Site-specific labeling of the constructs with [$^{99m}\text{Tc}(\text{CO})_3$] $^+$ was performed according to methods developed earlier^{14,20} with a radiochemical yield ranging from 50 to 84%. After labeling, a simple purification step was performed to remove unconjugated [$^{99m}\text{Tc}(\text{CO})_3$] $^+$ using disposable NAP-5 size-exclusion columns, resulting in a radiochemical purity of 97 to 99% for all constructs.

Table 3: *In vitro* stability of [$^{99m}\text{Tc}(\text{CO})_3$] $^+$ -labeled affibody molecules. The challenge was performed by incubation with 5000-fold molar excess of histidine at 37°C during 4 h. Control samples were kept at room temperature during the same time. The experiment was performed in duplicates. The data are presented as an average of the two experiments with maximum error.

	Protein-associated radioactivity, %	
	After histidine challenge	Control (PBS)
[$^{99m}\text{Tc}(\text{CO})_3$] $^+$ -(HE) $_3$ -Z _{HER2:342}	93.3±0.2	97.6±0.1
[$^{99m}\text{Tc}(\text{CO})_3$] $^+$ -Z _{HER2:342} -(HE) $_3$	75.8±0.6	86.6±1.0
[$^{99m}\text{Tc}(\text{CO})_3$] $^+$ -(HK) $_3$ -Z _{HER2:342}	99.15±0.05	99.8±0.1
[$^{99m}\text{Tc}(\text{CO})_3$] $^+$ -Z _{HER2:342} -(HK) $_3$	93.3±0.5	95.1±0.5
[$^{99m}\text{Tc}(\text{CO})_3$] $^+$ -(HA) $_3$ -Z _{HER2:342}	98.4±0.2	99.2±0.2
[$^{99m}\text{Tc}(\text{CO})_3$] $^+$ -Z _{HER2:342} -(HA) $_3$	83.4±1.5	91.8±0.5
[$^{99m}\text{Tc}(\text{CO})_3$] $^+$ -H $_6$ -Z _{HER2:342}	94.6±0.5	98.6±0.4
[$^{99m}\text{Tc}(\text{CO})_3$] $^+$ -Z _{HER2:342} -H $_6$	92.9±0.4	96.8±0.7
[$^{99m}\text{Tc}(\text{CO})_3$] $^+$ -(HI) $_3$ -Z _{HER2:342}	95.6±0.1	97.6±0.1
[$^{99m}\text{Tc}(\text{CO})_3$] $^+$ -Z _{HER2:342} -(HI) $_3$	87.3±1.2	95.8±0.7

To evaluate the stability of the radiolabel, the constructs were subjected to a histidine challenge where they were incubated with 5000-fold molar excess of histidine for 4 h (Table 3). The results show an appreciably higher stability of conjugates having the (HX)₃-tag in the N-terminus compared to the variants with the same tag in the C-terminus. The same pattern was also observed in the control experiments, where PBS without histidine was used. The retained radioactivity for all conjugates with N-terminal tags was higher than 97%. The nature of the non-histidine side chain also appeared to influence the stability. The positively charged HKHKHK-tag offered the most stable conjugate at both C- or N-terminal positioning compared to the other variants, whereas the least stable label was found for the negatively charged HEHEHE-tag for both positions.

Binding specificity of radiolabeled affibody molecules to HER2-expressing cells in vitro

To investigate the binding of the radiolabeled constructs to HER2 expressing cells, SKOV-3 cells were incubated with the constructs with or without pre-incubation with non-radiolabeled Z_{HER2:342}. The results are displayed in Table 4 and indicate that binding of [^{99m}Tc(CO)₃]⁺-(HA)₃-Z_{HER2:342}, [^{99m}Tc(CO)₃]⁺-Z_{HER2:342}-(HA)₃, [^{99m}Tc(CO)₃]⁺-(HK)₃-Z_{HER2:342}, [^{99m}Tc(CO)₃]⁺-Z_{HER2:342}-(HK)₃, [^{99m}Tc(CO)₃]⁺-(HI)₃-Z_{HER2:342}, [^{99m}Tc(CO)₃]⁺-Z_{HER2:342}-(HI)₃, and [^{99m}Tc(CO)₃]⁺-Z_{HER2:342}-(HE)₃ was receptor mediated since saturation of the receptors by pre-incubation with non-labeled Z_{HER2:342} significantly decreased binding. For [^{99m}Tc(CO)₃]⁺-(HI)₃-Z_{HER2:342}, an unusually high level of unspecific binding was detected, even though it also decreased upon pre-saturation of the receptors. Previously, a similar study on [^{99m}Tc(CO)₃]⁺-(HE)₃-Z_{HER2:342}, [^{99m}Tc(CO)₃]⁺-Z_{HER2:342}-H₆ and [^{99m}Tc(CO)₃]⁺-H₆-Z_{HER2:342} was performed,

where the results also indicated that cell binding was receptor mediated, since it could be decreased also for these constructs by receptor pre-saturation.²⁰

Table 4. Specificity of binding of [^{99m}Tc(CO)₃]⁺-labeled affibody molecules to HER2-expressing SKOV-3 cells in vitro^a

	Cell-bound radioactivity, %		
	non-		p-value
	blocked	blocked	
[^{99m} Tc(CO) ₃] ⁺ -(HA) ₃ -Z _{HER2:342}	21±2	0.78±0.06	< 5 x 10 ⁻⁵
[^{99m} Tc(CO) ₃] ⁺ -Z _{HER2:342} -(HA) ₃	27±1	0.56±0.04	< 5 x 10 ⁻⁶
[^{99m} Tc(CO) ₃] ⁺ -(HK) ₃ -Z _{HER2:342}	14.8±0.9	2.1±0.5	< 5 x 10 ⁻⁵
[^{99m} Tc(CO) ₃] ⁺ -Z _{HER2:342} -(HK) ₃	28±4	1.7±0.1	< 5 x 10 ⁻⁵
[^{99m} Tc(CO) ₃] ⁺ -(HI) ₃ -Z _{HER2:342}	12.4±0.3	7.3±0.2	0.0002
[^{99m} Tc(CO) ₃] ⁺ -Z _{HER2:342} -(HI) ₃	35±1	0.62±0.04	< 5 x 10 ⁻⁶
[^{99m} Tc(CO) ₃] ⁺ -Z _{HER2:342} -(HE) ₃	30±1	1.9±0.1	< 5 x 10 ⁻⁶

^aCells were incubated with 1 nM of radiolabeled conjugates for 1 h at 37°C. For pre-saturation of HER2, a 500-fold molar excess of non-radioactive affibody molecules was added. Data are presented as mean values of percent added radioactivity that is cell-bound from three cell dishes and standard deviations.”

In vivo studies

In order to determine the radioactivity uptake in different organs in vivo, the radiolabeled constructs were injected into female NMRI mice. Data concerning biodistribution, 4 and 24 h p.i., are presented in Table 5. For all 10 constructs, the biodistribution pattern was typical for affibody molecules, where clearance via glomeruli was rather fast, followed by renal re-absorption, except for [^{99m}Tc(CO)₃]⁺-(HI)₃-Z_{HER2:342} and [^{99m}Tc(CO)₃]⁺-(HK)₃-Z_{HER2:342}. The ratio of radioactivity uptake at 4 and 24 h p.i. in liver and kidneys was in the range of 1.5-2 for all conjugates,

indicating a moderately residualizing character of all constructs. The obtained biodistribution of $[^{99m}\text{Tc}(\text{CO})_3]^+(\text{HE})_3\text{-Z}_{\text{HER2:342}}$, $[^{99m}\text{Tc}(\text{CO})_3]^+\text{-Z}_{\text{HER2:342}}\text{-H}_6$, and $[^{99m}\text{Tc}(\text{CO})_3]^+\text{-H}_6\text{-Z}_{\text{HER2:342}}$ were in agreement with a previously published data for these constructs²⁰.

Table 5. Biodistribution of $[^{99m}\text{Tc}(\text{CO})_3]^+$ -labeled affibody molecules in female NMRI mice, 4 and 24 h after intravenous injection. The measured radioactivity of different organs is expressed as % ID/g, and presented as an average value from 4 animals \pm standard deviation.

	$\text{His}_6\text{-Z}_{\text{HER2:342}}$		$\text{Z}_{\text{HER2:342}}\text{-His}_6$	
	4 h	24 h	4 h	24 h
Blood	0.42 \pm 0.01	0.15 \pm 0.02	0.9 \pm 0.1	0.347 \pm 0.003
Lung	0.7 \pm 0.4	0.5 \pm 0.1	1.2 \pm 0.3	0.8 \pm 0.2
Liver	10.5 \pm 0.7	6.3 \pm 0.8	5 \pm 1	4.2 \pm 0.5
Spleen	1.22 \pm 0.06	1.0 \pm 0.1	0.8 \pm 0.2	0.9 \pm 0.2
Kidney	109 \pm 13	56 \pm 10	128 \pm 19	98 \pm 13
Muscle	0.17 \pm 0.01	0.09 \pm 0.01	0.23 \pm 0.04	0.17 \pm 0.04
Bone	0.56 \pm 0.1	0.38 \pm 0.05	0.7 \pm 0.2	0.6 \pm 0.1
GI tract ^a	8 \pm 2	1.6 \pm 0.5	4.1 \pm 0.6	2.0 \pm 0.4
Carccass ^a	5.3 \pm 0.3	2.7 \pm 0.2	7 \pm 1	5.3 \pm 0.7

	$(\text{HE})_3\text{-Z}_{\text{HER2:342}}$		$\text{Z}_{\text{HER2:342}}\text{-(HE)}_3$	
	4 h	24 h	4 h	24 h
Blood	0.83±0.06	0.20±0.03	2.4±0.2	0.6±0.2
Lung	0.80±0.07	0.3±0.1	2.0±0.2	0.7±0.2
Liver	1.5±0.1	0.8±0.2	3.9±0.4	2.3±0.3
Spleen	0.2±0.2	0.14±0.06	1.1±0.1	0.50±0.07
Kidney	129±15	57±6	117±10	61±9
Muscle	0.2±0.1	0.06±0.02	0.42±0.02	0.16±0.03
Bone	0.3±0.1	0.11±0.04	1.1±0.1	0.53±0.08
GI tract ^a	5±1	1.1±0.2	3.6±0.3	1.8±0.5
Carccass ^a	4.2±0.3	1.6±0.3	11.7±0.8	5.3±0.3

	$(\text{HK})_3\text{-Z}_{\text{HER2:342}}$		$\text{Z}_{\text{HER2:342}}\text{-(HK)}_3$	
	4 h	24 h	4 h	24 h
Blood	0.5±0.1	0.16±0.02	1.7±0.2	0.46±0.06
Lung	1.0±0.3	0.7±0.2	2.0±0.5	0.9±0.2
Liver	23±4	12±2	13±2	9±2
Spleen	2.5±0.5	1.7±0.4	1.5±0.1	0.8±0.2
Kidney	36±3	27±6	84±14	53±5
Muscle	0.15±0.03	0.09±0.01	0.38±0.02	0.19±0.03
Bone	0.8±0.1	0.6±0.2	0.92±0.06	0.6±0.1
GI tract ^a	7.4±0.6	1.9±0.4	3.6±0.3	2.8±0.5
Carccass ^a	6.0±0.9	3.1±0.3	11±5	6±1

	$(\text{HA})_3\text{-Z}_{\text{HER2}:342}$		$\text{Z}_{\text{HER2}:342}\text{-(HA)}_3$	
	4 h	24 h	4 h	24 h
Blood	0.40±0.09	0.13±0.03	1.8±0.1	0.50±0.08
Lung	0.5±0.1	0.316±0.009	2.7±0.2	1.0±0.1
Liver	4.2±0.8	2.8±0.3	4.1±0.4	2.8±0.3
Spleen	0.5±0.1	0.6±0.2	2.2±0.1	0.7±0.2
Kidney	78±8	51±9	116±16	63±5
Muscle	0.10±0.01	0.06±0.01	0.54±0.06	0.20±0.02
Bone	0.29±0.05	0.27±0.02	1.8±0.2	0.5±0.1
GI tract ^a	16±4	1.2±0.2	3.3±0.2	2.2±0.5
Carccass ^a	3.4±0.4	1.88±0.06	9.9±0.9	5.1±0.6

	$(\text{HI})_3\text{-Z}_{\text{HER2}:342}$		$\text{Z}_{\text{HER2}:342}\text{-(HI)}_3$	
	4 h	24 h	4 h	24 h
Blood	1.09±0.02	0.3±0.1	1.2±0.1	0.43±0.03
Lung	7.3±1.0	2.1±0.3	1.5±0.4	0.9±0.2
Liver	32±4	19±6	6.4±0.8	3.6±0.6
Spleen	38±9	14±3	0.9±0.2	0.7±0.1
Kidney	9±2	6±2	106±8	56±6
Muscle	0.19±0.06	0.11±0.02	0.30±0.06	0.16±0.04
Bone	0.7±0.4	0.39±0.08	0.8±0.2	0.46±0.06
GI tract ^a	4.3±0.4	3±1	6±2	2.0±1.0
Carccass ^a	5.7±0.5	3.2±0.6	9±1	4.8±1.0

^adata for GI tract with content and carcass are presented as % of injected radioactivity per whole sample.

Overall, the analysis demonstrated a profound influence of the composition and position of the $(\text{HX})_3$ -tag on the measured biodistribution. Most obvious was the influence on uptake in liver and spleen, and the level of hepatobiliary excretion (Figure 3). From Figure 3, it is apparent that

positioning of the tags was crucial. For C-terminal placement, the radioactivity uptake in liver was significantly higher for $[^{99m}\text{Tc}(\text{CO})_3]^+$ -Z_{HER2:342}-(HK)₃ than for the other four constructs (Figure 3B). However, the difference between the other variants was small. For N-terminal placement, the composition had a much more pronounced effect on biodistribution (Figure 3A). Incorporation of the lipophilic isoleucine in the tag shifted the excretion pathway from renal to hepatobiliary, and provoked a high uptake in spleen. Hydrophilic histidine and intermediate lipophilic alanine had elevated liver uptake, 10.5±0.7 and 4.2±0.8 % ID/g at 4 h p.i., respectively. Although hepatic uptake per gram tissue was lower for $[^{99m}\text{Tc}(\text{CO})_3]^+$ -(HA)₃-Z_{HER2:342}, more radioactivity was excreted through bile into GI-tract. The sum of radioactivity (% ID per whole organ) in liver plus GI-tract did not differ significantly between $[^{99m}\text{Tc}(\text{CO})_3]^+$ -(HA)₃-Z_{HER2:342} (20.9±4.5 % ID) and $[^{99m}\text{Tc}(\text{CO})_3]^+$ -H₆-Z_{HER2:342} (22.1±2.9% ID).

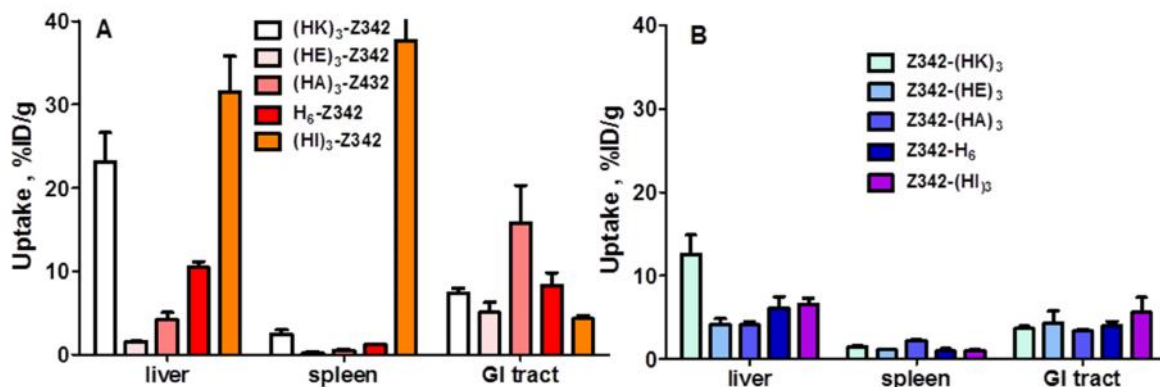


Figure 3. Influence of position and composition of the (HX)₃-tag on uptake of $[^{99m}\text{Tc}(\text{CO})_3]^+$ -labeled affibody molecules in liver, spleen and gastrointestinal tract at 4 after injection. A. (HX)₃-tags placed in the N-terminus. B. (HX)₃-tags placed in the C-terminus.

The radioactivity of different organs is expressed as % ID/g, and presented as an average value from 4 animals ± standard deviation.

* data for intestines with content are presented as % of injected radioactivity per whole sample.

The conjugate with the hydrophilic glutamate ($[^{99m}\text{Tc}(\text{CO})_3]^+-(\text{HE})_3\text{-Z}_{\text{HER2:342}}$) had the lowest uptake in liver and lowest sum of hepatic uptake and hepatobiliary excretion. Surprisingly, $[^{99m}\text{Tc}(\text{CO})_3]^+-(\text{HK})_3\text{-Z}_{\text{HER2:342}}$ had high uptake in both liver and spleen, although lysine is considered to be as hydrophilic as glutamate (Figure 1).^{21,22}

The influence of position and composition of the $(\text{HX})_3$ -tags on radioactive concentration in blood, as well as in lung and muscle was very distinct (Figure 4A). The concentration of radioactivity in blood was lower for conjugates with N-terminal placement of the tag compared to conjugates with C-terminal placement. The pattern was similar for lungs (except for $[^{99m}\text{Tc}(\text{CO})_3]^+-(\text{HI})_3\text{-Z}_{\text{HER2:342}}$) and muscle. There was a good correlation between concentration of radioactivity in blood at 4 h p.i. and release of radioactivity during the histidine challenge (Figure 4B).

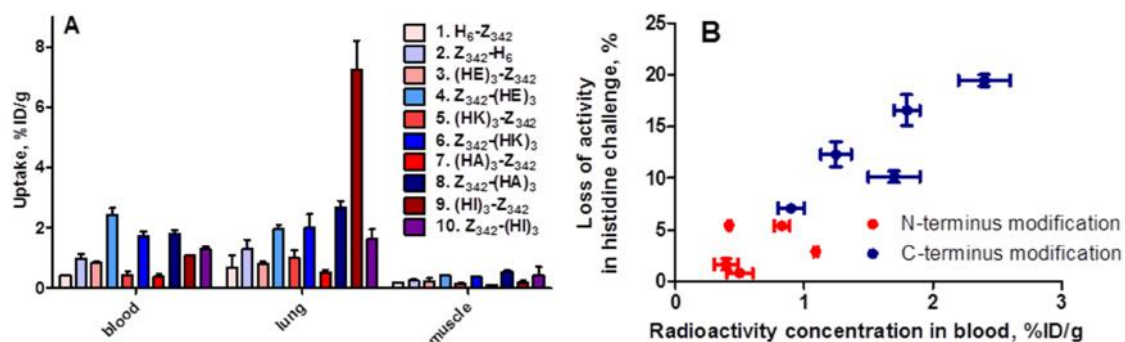


Figure 4. A. Influence of position and composition of the $(\text{HX})_3$ -tags on radioactivity concentration of $[^{99m}\text{Tc}(\text{CO})_3]^+$ -labeled affibody molecules in blood, lung and muscle at 4 p.i.. The concentration of radioactivity in different organs is expressed as % ID/g, and presented as an average value from 4 animals \pm standard deviation. B. Correlation between release of radioactivity from $[^{99m}\text{Tc}(\text{CO})_3]^+$ -labeled affibody molecules during histidine challenge and radioactivity concentration in blood at 4 h p.i.

DISCUSSION AND CONCLUSION

The use of a built-in tag in a recombinantly expressed affinity protein for both purification and labeling with $[^{99m}\text{Tc}(\text{CO})_3]^+$ is convenient. However, tagging the HER2 binding affibody molecule $Z_{\text{HER2:342}}$ with the commonly used N-terminal hexa-histidine tag (H_6 -tag) was found to be associated with high liver uptake.^{14,20} Furthermore, it was previously shown that the presence of a H_6 -tag in the N-terminus is associated with a substantially elevated liver uptake when nuclides, other than ^{99m}Tc , were attached to the C-terminus.^{23,24} A previous study demonstrated that the liver uptake of $[^{99m}\text{Tc}(\text{CO})_3]^+$ -labeled affibody molecules could be substantially reduced by replacing every second histidine in the tag by the hydrophilic glutamate resulting in the HEHEHE-tag or by repositioning the H_6 -tag to the C-terminus.²⁰ At the same time, the tumor uptake was not influenced by the composition of histidine-containing tag (no significant difference between tested conjugates).²⁰ This translates into a much higher tumor-to-liver ratio, which could potentially enable imaging of liver metastases in clinics in the future.²⁰

Furthermore, a similar effect (i.e. high tumor-to-liver ratio) as a result of the composition of an N-terminally placed histidine-containing tag was observed for other kinds of residualizing labels placed in the C-terminus, such as ^{111}In attached to the affibody molecule using the DOTA chelator or $^{99m}\text{Tc}=\text{O}$ attached via a cysteine-containing peptide based chelator.²⁵ A reduction of liver uptake was also observed for an IGF-1R binding affibody molecule conjugated with $[^{99m}\text{Tc}(\text{CO})_3]^+$ using an N-terminal HEHEHE-tag compared to the same construct with a H_6 -tag.²⁶

Still, it was impossible to determine all major factors that influence liver uptake. In other studies, positive correlation between lipophilicity and hepatic uptake were observed for different targeting proteins and peptides.²⁷ Thus, a combination of the lipophilic $[^{99m}\text{Tc}(\text{CO})_3]^+$ and deprotonated histidines might be an explanation for the increase. However, the liver uptake of affibody molecules with a N-terminal hexa-histidine tag is high even in the absence of the $[^{99m}\text{Tc}(\text{CO})_3]^+$ -

label.²³⁻²⁵ Another contributing factor might be the charge of the tag. Studies on biodistribution of affibody molecules labeled with $^{99m}\text{Tc}=\text{O}$ using peptide-based chelators demonstrated that the presence of a lysine in the chelator causes high liver uptake for both N-terminal²⁸ and C-terminal^{16,17} positioning of the label. In fact, high liver uptake of both $^{99m}\text{Tc}-(\text{HK})_3\text{-Z}_{\text{HER2:342}}$ and $^{99m}\text{Tc-Z}_{\text{HER2:342}}-(\text{HK})_3$, which was observed in this study, suggests that a positive charge in the histidine-containing tag plays a substantial role. However, the influence of lipophilicity was also obvious. For the N-terminally placed and lipophilic (HI)₃-tag, liver uptake and hepatobiliary excretion was higher than for the hydrophilic (HE)₃-tag. For $[^{99m}\text{Tc}(\text{CO})_3]^+(\text{HA})_3\text{-Z}_{\text{HER2:342}}$ and $[^{99m}\text{Tc}(\text{CO})_3]^+\text{-H}_6\text{-Z}_{\text{HER2:342}}$, the sum of liver uptake and hepatobiliary excretion was the same, but $^{99m}\text{Tc-H}_6\text{-Z}_{\text{HER2:342}}$ had higher hepatic retention in contrast to $[^{99m}\text{Tc}(\text{CO})_3]^+(\text{HA})_3\text{-Z}_{\text{HER2:342}}$, which had a higher hepatobiliary excretion. This suggests that the hepatocytes handled these constructs or their radiocatabolites differently. Together, these data indicate that the hepatic uptake of affibody molecules occurs by two different pathways. One is promoted by positive charge and the other by lipophilicity. Uptake in the kidneys of the variants with an N-terminal (HX)₃-tag was inversely correlated with the uptake in the liver which indicates that renal excretion, which is otherwise typical for the $\text{Z}_{\text{HER2:342}}$ affibody molecule, was suppressed by hepatic uptake. An important conclusion from this study is that an increase in hydrophilicity of the (HX)₃-tags improves the biodistribution of the affibody molecules but lysine, and possibly other positively charged amino acids, appears to be undesirable in the chelator of ^{99m}Tc .

An interesting observation is the influence of positioning of the tags on biodistribution. The effect of the composition of the tag can be observed also for C-terminal placement, but it was much less pronounced than for N-terminal positioning (Figure 3). This is in agreement with the earlier observations that modification of the C-terminus of affibody molecules has smaller impact on

hepatic uptake and hepatobiliary excretion.¹⁶ It is also concordant with the idea that not only overall lipophilicity, but also local concentration of surface-exposed lipophilic amino acids ("lipophilic patches") might be a contributing factor for elevated liver uptake.²⁹ It should be noted that the N-terminus is located close to the target-binding site containing a number of surface-exposed hydrophobic amino acids. In a previous study it was demonstrated that the composition of the binding site can influence the biodistribution pattern of affibody molecules affecting their blood clearance rate and liver uptake.³⁰ It is therefore not surprising that N-terminally placed lipophilic histidine containing tags gives rise to higher liver uptake than the same tags in the C-terminus, and is possibly a consequence of their closeness to the lipophilic amino acids in the binding site.

An important finding of this study is that the blood concentration and uptake in lung and muscle was lower for affibody molecules having (HX)₃-tags in the N-terminus with the exception of [^{99m}Tc(CO)₃]⁺-(HI)₃-Z_{HER2:342} (Figure 4A). The lipophilicity of the conjugates might cause an elevated stickiness to blood plasma proteins increasing its retention in blood, but there was no correlation between blood concentration and the hydrophobicity of the tags. Instead, there was a strong correlation between loss of activity from conjugates during the histidine challenge and radioactivity concentration in the blood (Figure 4B). There was a report that surrounding amino acids influence the stability of histidine-based tags³¹ and it is likely, that the same effect was observed also in this study. Weakly bound [^{99m}Tc(CO)₃]⁺ can transchelate to blood proteins, which would slow down the clearance of radioactivity. The higher uptake in lung and muscle could then be a consequence of the higher blood concentration of radioactivity. An important practical implication is that the use of C-terminal tags is unfavorable for affibody molecules intended for labeling with [^{99m}Tc(CO)₃]⁺.

Radionuclide molecular imaging might be a powerful tool to help in personalizing cancer treatment. Particularly, imaging of membranous expression of molecular targets, such as RTKs, is a promising approach. An important factor for successful imaging is a high sensitivity, which depends on high contrast between the targeted structures and surrounding tissue. The use of small (4-10k Da) scaffold proteins as imaging agents provides a combination of rapid in vivo kinetics and high affinity that creates a pre-condition for high contrast in vivo imaging.³² Our studies also suggest that selection of labeling chemistry (radionuclide, chelator/linker, labeling and purification conditions) is as critical for successful imaging as selection of the affinity protein.

In conclusion, the current study demonstrates that the glutamate-containing (HX)₃-tag, located in the N-terminus, is the preferable choice for purification and labeling of affibody molecules with [^{99m}Tc(CO)₃]⁺. The use of this tag can simplify development of affibody molecules for radionuclide molecular imaging of a variety of molecular targets. It will hopefully aid in the development of other scaffold proteins as well.

EXPERIMENTAL SECTION

General

The purity of each peptide was analyzed by RP-HPLC on a Reprosil Gold 300 C18 column (4.6 x 250 mm, 3 μ m particle size (Dr Maisch, Ammerbuch, Germany)) using a gradient of 20-50% B (A: 0.1% trifluoroacetic acid (TFA) in H₂O and B: 0.1% TFA in acetonitrile) over 20 minutes using a flow rate of 1 mL/min. From each recorded chromatogram, the integrated peak area corresponding to the affibody molecule at 220 nm was divided by to the area of all peaks using Chemstation software (Agilent Technology) to measure the purity. The purity was found to be >95% for all peptides. IsoLink kits were kindly provided by Covidien (Mansfield, MA, USA). Buffers were prepared using common methods from chemicals supplied by Merck (Darmstadt, Germany). High-quality Milli-Q water (resistance higher than 18 M Ω /cm) was used for preparing solutions. ^{99m}Tc was obtained as pertechnetate from an Ultra-TechneKow generator (Covidien) by elution with sterile 0.9 % NaCl. NAP-5 size exclusion columns were from GE Healthcare (Uppsala, Sweden). 0.1 M phosphate buffered saline (PBS), pH 7.5 was prepared using common methods. Cells used during *in vitro* experiments were detached using a trypsin-EDTA solution (0.25% trypsin, 0.02% EDTA in buffer, Biochrom AG, Berlin, Germany). For *in vivo* experiments Ketalar (50 mg/mL, Pfizer, NY, USA), Rompun (20 mg/mL, Bayer, Leverkusen, Germany) and Heparin (5000 IE/mL, Leo Pharma, Copenhagen, Danmark) were used. Data on cellular uptake and biodistribution were assessed by an unpaired, two-tailed *t*-test using GraphPad Prism (version 4.00 for Windows GraphPad Software, San Diego, CA, USA) in order to determine any significant differences (p<0.05). Radioactivity was measured using an automated gamma-counter with a 3-inch NaI(Tl) detector (1480 WIZARD, Wallac Oy, Turku, Finland). The distribution of radioactivity along thin layer chromatography strips and SDS-PAGE

gels was measured on a Cyclone™ Storage Phosphor System and analyzed using the OptiQuant™ image analysis software (PerkinElmer, Waltham, MA, USA).

The net charges of the tags at pH=7.0 were calculated at <http://www.innovagen.se/custom-peptide-synthesis/peptide-property-calculator/peptide-property-calculator.asp> as described.³³ The grand averages of hydrophathy (GRAVY-score) of the tags at pH=7.0 were calculated at <http://web.expasy.org/protparam/> using the methods described by Kyte *et al.*²¹

The gene coding for the affibody molecule Z_{HER2:342} was PCR amplified using DNA primers carrying overhang-extensions encoding the different (HX)₃-tags, HHHHHH, HEHEHE, HAHAHA, HKHKHK or HIHIHI. The resulting DNA fragments were cut with HindIII (New England Biolabs, Ipswich, MA, USA) and NdeI (New England Biolabs) followed by ligation using T4 DNA ligase (New England Biolabs) into the protein expression vector pET21a(+) (Novagen, Darmstadt, Germany). Correct DNA sequences were verified by DNA sequencing. The different Z_{HER2:342} variants were produced in *Escherichia coli* strain BL21(DE3) after inducing protein expression by adding isopropyl-β-D-1-thiogalactopyranoside (IPTG) to a final concentration of 1.0 mM. After 4 h of production (37°C, 125 rpm), cells were harvested by centrifugation (2200xg, 10 min, 4°C), and resuspended in wash buffer (50 mM H₂PO₄, 300 mM NaCl, pH 7.5). Cells were disrupted by sonication and cell debris was removed by centrifugation (35 000xg, 20 min, 4°C). Finally, the clarified cell lysate was filtered through a 0.45 μm filter (Merck Millipore, Billerica, MA, USA), before applied onto a Talon metal affinity resin (BD Bioscience, San Jose, CA, USA), except for (HI)₃-Z_{HER2:342} which was applied to a Ni²⁺-chelating sepharose resin (GE Healthcare). After extensive washing, the affibody variants were eluted using elution buffer (50 mM NaAc, 300 mM NaCl, pH 5.0).

The affibody constructs were further purified by reverse-phase high performance liquid chromatography (RP-HPLC) on an Agilent 1200 instrument (Agilent Technology, Santa Clara, CA, USA) using a Reprosil Gold 300 C18 column (10 x 250 mm, 5 μ m particle size, Dr Maisch). Elution was carried out by applying a gradient of 20-50% B (A: 0.1% TFA in H₂O and B: 0.1% TFA in acetonitrile) over 20 minutes using a flow rate of 2.5 mL/min.

Characterization of affibody molecules

The molecular masses of the Z_{HER2:342} constructs were determined on a 6520 Accurate-Mass Q-TOF LC-MS instrument (Agilent Technologies), using Agilent *MassHunter* software (Agilent Technologies) to interpret the isotopic and charge state information. Variable temperature measurements (VTM) were performed on a JASCO J-810 spectropolarimeter instrument (JASCO, Tokyo, Japan). 60 μ M of each affibody molecule, diluted in PBS was subjected to a temperature gradient increasing 5°C/min from 20 to 90°C while measuring the signal at 221 nm. To investigate the impact on secondary structure as a consequence of heat-treatment, circular dichroism spectra from 250 to 195 nm were recorded at 20°C before and after heating to 90°C. In order to determine if the (HX)₃-tags' composition and location influenced the binding affinity of Z_{HER2:342} to HER2, real-time biosensor analysis on a BIAcore3000 instrument (GE Healthcare) was performed. 800 RU of the extracellular domain of HER2 fused to the Fc region of human IgG (R&D systems, Minneapolis, MN, USA) was immobilized on a flow-cell surface of a CM5 chip (GE Healthcare) by amine coupling according to manufacturer's recommendation. As a reference, another flow-cell surface was activated and deactivated without any immobilization. A three-fold dilution series comprised of three different concentrations ranging between 10-1.1 nM was prepared for each (HX)₃-Z_{HER2:342} variant. Samples were injected over the flow-cell using a

flow rate of 50 $\mu\text{L}/\text{min}$ with 5 min association and 20 min dissociation before regenerating the flow-cell surfaces with 20 μL of 20 mM HCl. All concentrations were run in duplicates. The association constant (k_a), the dissociation constant (k_d) and the equilibrium dissociation constant (K_D), were retrieved using the BIAcore evaluation software *BIAeval* applying a global curve fit and assuming a one-to-one interaction model.

Labeling of affibody molecules with [$^{99\text{m}}\text{Tc}(\text{CO})_3$] $^+$

Labeling of affibody molecules with [$^{99\text{m}}\text{Tc}(\text{CO})_3$] $^+$ was performed as described earlier.^{14,20} Briefly, 500 μL (350 MBq-2 GBq) of $^{99\text{m}}\text{TcO}_4^-$ -containing generator eluate were added to a vial with the IsoLink kit. The mixture was incubated at 100°C for 20 min. Thereafter, 40 μL of mixture was transferred to a tube containing 50 μg (~6.8 nmol) affibody molecule in 40 μL PBS followed by incubation at 50°C. The labeling yield after incubation for 60 min was monitored by ITLC. 1 μL samples were taken for analysis of the labeling yield using 150-771 DARK GREEN strips eluted with PBS. When the ITLC strips were eluted with PBS, pertechnetate, as well as carbonyl and histidine complexes of $^{99\text{m}}\text{Tc}$ migrated with the eluent front ($R_f = 1.0$), while affibody molecules do not move under these conditions ($R_f = 0.0$). The experiments were performed in quadruplicates. In addition, blank experiments were performed, where the affibody molecules were omitted. The labeled affibody molecules were purified using NAP-5 desalting columns (GE Healthcare), pre-equilibrated and eluted with PBS. The purity of each preparation was evaluated using thin layer chromatography.

To evaluate the stability of the $^{99\text{m}}\text{Tc}$ -label, a histidine challenge of the conjugates was performed.¹⁸ Samples of each labeled conjugate were incubated at 37°C with 5000-fold excess of

histidine for 5 h. Control samples were incubated at 20°C in PBS. Thereafter, the samples were analyzed using ITLC as described above.

Binding specificity of radiolabeled affibody molecules to HER2-expressing cells in vitro

The specificity of binding of the radiolabeled affibody molecules to HER2-expressing cells in vitro was evaluated as previously described.²⁰ The SKOV-3 ovarian carcinoma cell line (American Type Tissue Culture Collection (ATCC) via LGC Promochem, Borås, Sweden) was used for the test. Labeled conjugates were added to cell dishes in concentrations of 1 nM. To one set of dishes non-labeled Z_{HER2:342} at a concentration of 0.5 μM was added 30 min before the labeled conjugate to saturate receptors on cells. The total volume of solutions was 1 mL and the experiment was done in triplicates. Cells were incubated for 1 h at 37°C, after which the medium was collected. The cells were washed once with cold serum-free medium, followed by detachment with 0.5 mL trypsin-EDTA. The cells were subsequently resuspended in 0.5 mL complete medium and collected. The radioactivity of the incubation medium and the cells was measured and the percent of cell-bound radioactivity was determined for each set of samples.

In vivo studies

All animal experiments were planned and performed in accordance with the national legislation on laboratory animals' protection and were approved by the Local Ethics Committee for Animal Research.

Female NMRI mice (18 weeks old, weight 24-29g) were used in the biodistribution studies. The biodistribution of each conjugate was determined at 4 or 24 h after injection. A group of four

mice was used for each data point. The animals were intravenously injected with 70 kBq (for measurement at 4 h p.i.) or 640 kBq (for measurement at 24 h p.i.) of radiolabeled conjugate diluted in 100 μ L PBS. In each case, the injected protein dose was adjusted with non-labeled affibody molecule to 1 μ g (0.12 nmol) per mouse. The mice were euthanized at 4 h or 24 h after injection by an intraperitoneal injection of Ketalar Rompun solution (20 μ L of solution per gram body weight: Ketalar, 10 mg/mL; Rompun, 1 mg/mL) followed by heart puncture with a 1 mL syringe rinsed with Heparine (5000 IE/mL). Blood and organ samples: lung, liver, spleen, kidneys, muscle, bone, intestines (with content) and the remaining carcass were collected, weighed and their radioactivity was measured. The organ uptake values are expressed as percent of injected dose per gram of tissue (% ID/g), except for the intestines and the remaining carcass where values are expressed as % ID per whole sample.

ANCILLIARY INFORMATION

Corresponding author information: +46-8-5537 8332, torbjorn@biotech.kth.se

Acknowledgements: This research was financially supported by grants from Swedish Cancer Society (Cancerfonden), Swedish Research Council (Vetenskapsrådet). Authors express their gratitude to Covidien for providing IsoLink kits.

Abbreviations used: GRAVY, Grand average of hydropathy; H₆, Hexa-histidine; IMAC, Immobilized metal-ion affinity chromatography; IPTG, isopropyl-β-D-1-thiogalactopyranoside; LC-MS, Liquid chromatography-mass spectrometry; PBS, Phosphate buffered saline; RP-HPLC, Reverse-phase high performance liquid chromatography; RTK, Receptor tyrosine kinase; TFA, trifluoroacetic acid

REFERENCES

- (1) Sharma, P.S.; Sharma, R.; Tyagi, T. Receptor tyrosine kinase inhibitors as potent weapons in war against cancers. *Curr. Pharm. Des.* **2009**, *15*, 758-776.
- (2) Tolmachev, V.; Stone-Elander, S.; Orlova, A. Current approaches to the use of radiolabeled tyrosine kinase-targeting drugs for patient stratification and treatment response monitoring: prospects and pitfalls. *Lancet Oncol.* **2010**, *11*, 992-1000.
- (3) Löfblom, J.; Feldwisch, J.; Tolmachev, V.; Carlsson, J.; Ståhl, S.; Frejd, F.Y. Affibody molecules: engineered proteins for therapeutic, diagnostic and biotechnological applications. *FEBS Lett.* **2010**, *584*, 2670-2680.
- (4) Orlova, A.; Magnusson, M.; Eriksson, T. L.; Nilsson, M.; Larsson, B.; Höiden-Guthenberg, I.; Widström, C.; Carlsson, J.; Tolmachev, V.; Ståhl, S.; Nilsson, F. Y. Tumor imaging using a picomolar affinity HER2 binding Affibody molecule. *Cancer Res.* **2006**, *66*, 4339-4348.
- (5) Tolmachev, V.; Rosik, D.; Wållberg, H.; Sjöberg, A.; Sandström, M.; Hansson, M.; Wennborg, A.; Orlova, A. Imaging of EGFR expression in murine xenografts using site-specifically labeled anti-EGFR ¹¹¹In-DOTA-Z_{EGFR:2377} Affibody molecule: aspect of the injected tracer amount. *Eur. J. Nucl. Med. Mol. Imaging* **2010**, *37*, 613-622.
- (6) Kronqvist, N.; Malm, M.; Göstring, L.; Gunneriusson, E.; Nilsson, M.; Höiden-Guthenberg, I.; Gedda, L.; Frejd, F. Y.; Ståhl, S.; Löfblom, J. Combining phage and staphylococcal surface display for generation of ErbB3-specific Affibody molecules. *Protein Eng. Des. Sel.* **2010**, *24*, 385-396.
- (7) Lindborg, M.; Cortez, E.; Höiden-Guthenberg, I.; Gunneriusson, E.; von Hage, E.; Syud, F.; Morrison, M.; Abrahmsén, L.; Herne, N.; Pietras, K.; Frejd, F. Y. Engineered high-affinity Affibody molecules targeting platelet-derived growth factor receptor beta in vivo. *J. Mol. Biol.* **2011**, *407*, 298-315.

- (8) Tolmachev, V.; Malmberg, J.; Hofström, C.; Abrahmsén, L.; Bergman, T.; Sjöberg, A.; Sandström, M.; Gräslund, T.; Orlova, A. Imaging of insulin-like growth factor type 1 receptor in prostate cancer xenografts using the Affibody molecule ^{111}In -DOTA-Z_{IGF1R:4551}. *J. Nucl. Med.* **2012**, *53*, 90-97.
- (9) Ahlgren, S.; Tolmachev, V. Radionuclide molecular imaging using Affibody molecules. *Curr. Pharm. Biotechnol.* **2010**, *11*, 581-589.
- (10) Baum, R. P.; Prasad, V.; Müller, D.; Schuchardt, C.; Orlova, A.; Wennborg, A.; Tolmachev, V.; Feldwisch, J. Molecular imaging of HER2-expressing malignant tumors in breast cancer patients using synthetic ^{111}In - or ^{68}Ga -labeled Affibody molecules. *J. Nucl. Med.* **2010**, *51*, 892-897.
- (11) Sandberg, D.; Wennborg, A.; Feldwisch, F.; Tolmachev, V.; Carlsson, J.; Garske, U.; Sörensen, J.; Lindman, H. First clinical observations of HER2 specific [^{111}In]ABY-025 metastatic detection capability in females with metastatic breast cancer. *J. Nucl. Med.* **2012**, *53* (Supplement 1), 220.
- (12) Tolmachev, V.; Orlova, A. Influence of labeling methods on biodistribution and imaging properties of radiolabelled peptides for visualization of molecular therapeutic targets. *Curr. Med. Chem.* **2010**, *17*, 2636-2655.
- (13) Núñez, R.; Erwin, W. D.; Wendt, R. E.; Stachowiak, A.; Mar, M.; Stevens, D.; Madewell, J.E.; Yeung, H.W.; Macapinlac, H.A. Acquisition parameters for oncologic imaging with a new SPECT/multislice CT scanner. *Mol Imaging Biol.* **2010**, *2*, 110-138.
- (14) Orlova, A.; Nilsson, F. Y.; Wikman, M.; Widström, C.; Ståhl, S.; Carlsson, J.; Tolmachev, V. Comparative in vivo evaluation of technetium and iodine labels on an anti-HER2 Affibody for single-photon imaging of HER2 expression in tumors. *J. Nucl. Med.* **2006**, *47*, 512-519.

- (15) Tran, T. A.; Rosik, D.; Abrahmsén, L.; Sandström, M.; Sjöberg, A.; Wållberg, H.; Ahlgren, S.; Orlova, A.; Tolmachev, V. Design, synthesis and biological evaluation of a HER2-specific Affibody molecule for molecular imaging. *Eur. J. Nucl. Med. Mol. Imaging* **2009**, *36*, 1864-1873.
- (16) Wållberg, H.; Orlova, A.; Altai, M.; Hosseinimehr, S. J.; Widström, C.; Malmberg, J.; Ståhl, S.; Tolmachev, V. Molecular design and optimization of ^{99m}Tc -labeled recombinant Affibody molecules improves their biodistribution and imaging properties. *J. Nucl. Med.* **2011**, *52*, 461-469.
- (17) Altai, M.; Wållberg, H.; Orlova, A.; Rosestedt, M.; Hosseinimehr, S. J.; Tolmachev, V.; Ståhl, S. Order of amino acids in C-terminal cysteine-containing peptide-based chelators influences cellular processing and biodistribution of ^{99m}Tc -labeled recombinant Affibody molecules. *Amino Acids* **2012**, *42*, 1975-1985.
- (18) Waibel, R.; Alberto, R.; Willuda, J.; Finnern, R.; Schibli, R.; Stichelberger, A.; Egli, A.; Abram, U.; Mach, J. P.; Plüchthun, A.; Schubiger, P. A. Stable one-step technetium-99m labeling of His-tagged recombinant proteins with a novel Tc(I)-carbonyl complex. *Nat. Biotechnol.* **1999**, *17*, 897-901.
- (19) Novak-Hofer, I.; Waibel, R.; Zimmermann, K.; Schibli, R.; Grünberg, J.; Chester, K. A.; Murray, A.; Lo, B. K.; Perkins, A. C.; Schubiger, P. A. Radiometal labeling of antibodies and antibody fragments for imaging and therapy. *Methods Mol. Biol.* **2004**, *248*, 481-494.
- (20) Tolmachev, V.; Hofström, C.; Malmberg, J.; Ahlgren, S.; Hosseinimehr, S. J.; Sandström, M.; Abrahmsén, L.; Orlova, A.; Gräslund, T. HEHEHE-tagged Affibody molecules may be purified by IMAC, are conveniently labeled with $[\text{}^{99m}\text{Tc}(\text{CO})_3]^+$, and show improved biodistribution. *Bioconjug. Chem.* **2010**, *21*, 2013-2022.

- (21) Hopp, T. P.; Woods, K. R. Prediction of protein antigenic determinants from amino acid sequence. *Proc. Natl. Acad. Sci. U.S.A.* **1982**, *78*, 3824-3828.
- (22) Kyte, J.; Doolittle, R. F. A simple method for displaying the hydropathic character of a protein. *J. Mol. Biol.* **1982**, *157*, 105-132.
- (23) Ahlgren, S.; Orlova, A.; Rosik, D.; Sandström, M.; Sjöberg, A.; Baastrup, B.; Widmark, O.; Fant, G.; Feldwisch, J.; Tolmachev, V. Evaluation of maleimide derivative of DOTA for site-specific labeling of recombinant Affibody molecules. *Bioconjug. Chem.* **2008**, *19*, 235-243.
- (24) Ahlgren, S.; Wållberg, H.; Tran, T. A.; Widström, C.; Hjertman, M.; Abrahmsén, L.; Berndorff, D.; Dinkelborg, L. M.; Cyr, J. E.; Feldwisch, J.; Orlova, A.; Tolmachev, V. Targeting of HER2-expressing tumors with a site-specifically ^{99m}Tc -labeled recombinant Affibody molecule, Z_{HER2:2395}, with C-terminally engineered cysteine. *J. Nucl. Med.* **2009**, *50*, 781-789.
- (25) Hofström, C.; Orlova, A.; Altai, M.; Wangsell, F.; Gräslund, T.; Tolmachev, V. Use of a HEHEHE purification tag instead of a hexa-histidine tag improves biodistribution of Affibody molecules site-specifically labeled with ^{99m}Tc , ^{111}In , and ^{125}I . *J. Med. Chem.* **2011**, *54*, 3817-3826.
- (26) Orlova, A.; Hofström, C.; Strand, J.; Varasteh, Z.; Sandström, M.; Andersson, K.; Tolmachev, V.; Gräslund, T. [$^{99m}\text{Tc}(\text{CO})_3$]⁺-(HE)₃-Z_{IGF1R:4551}, a new Affibody conjugate for visualization of insulin-like growth factor-1 receptor expression in malignant tumours. *Eur. J. Nucl. Med. Mol. Imaging* **2013**, *40*, 439-449
- (27) Hosseinimehr, S. J.; Tolmachev, V. Orlova A. Liver uptake of radiolabeled targeting proteins and peptides: considerations for targeting peptide conjugate design. *Drug Discov. Today* **2012**, *17*, 1224-1232.
- (28) Tran, T.; Ekblad, T.; Orlova, A.; Widström, C.; Feldwisch, J.; Wennborg, A.; Abrahmsén, L.; Tolmachev, V.; Eriksson-Karlström, A. Effects of Lysine-containing mercaptoacetyl-based

Chelators on the Biodistribution of ^{99m}Tc -labeled anti-HER2 Affibody molecules. *Bioconjug. Chem.* **2008**, *19*, 2568-2576.

(29) Rusckowski, M.; Qu, T.; Gupta, S.; Ley, A.; Hnatowich, D. J. A comparison in monkeys of ^{99m}Tc labeled to a peptide by 4 methods. *J. Nucl. Med.* **2001**, *42*, 1870-1877.

(30) Tolmachev, V.; Tran, T. A.; Rosik, D.; Sjöberg, A.; Abrahmsén, L.; Orlova, A. Tumor targeting using Affibody molecules: interplay of affinity, target expression level, and binding site composition. *J. Nucl. Med.* **2012**, *53*, 953-960.

(31) Williams, J. D.; Cooper, M.; Kampmeier, F.; Tavaré, R.; Gmullen, G. E.; Blower, P. Novel His-tag Sequence for Highly Efficient Site-Specific Radiolabelling of Proteins with $[\text{}^{99m}\text{Tc}(\text{CO})_3]^+$ and $[\text{}^{186/188}\text{Re}(\text{CO})_3]^+$. *Eur. J. Nucl. Med. Mol Imaging* **2012**, *39* (supplement 2), S216.

(32) Miao, Z.; Levi, J.; Cheng, Z. Protein scaffold-based molecular probes for cancer molecular imaging. *Amino Acids.* **2011**, *41*, 1037-1047.

(33) Nelson, D. L.; Cox, M. M. *Lehninger Principles of Biochemistry*, 5:th ed.; W. H. Freeman and Company: New York, 2008

TABLE OF CONTENTS GRAPHICS

